Second law analysis of Giesekus viscoelastic fluid for axial annular flow

Mehdi Moayed Mohseni and Fariborz Rashidi*

Chemical Engineering Department,
Amirkabir University of Technology,
P.O. Box 15875-4413,
No. 472, Hafez Ave., Tehran, Iran
Fax: +98 21 6405847
Email: m.moayed@aut.ac.ir
Email: rashidi@aut.ac.ir
*Corresponding author

Abstract: The first and second laws of thermodynamics are analysed for viscoelastic fluid obeying Giesekus constitutive equation in concentric annulus under steady, laminar flow with both thermal and hydrodynamic fully developed conditions. Two types of boundary conditions are employed in this study. (a) Uniform heat flux is imposed at outer cylinder and insulated condition is considered for inner cylinder. (b) Both cylinders are kept at different constant temperatures. Governing equations in cylindrical coordinate system are simplified and then solved to obtain analytical expressions for temperature profile (Θ), entropy generation number (N_S) and Bejan number (Be). The effect of group parameter (Br/Ω), Brinkman number (Br), Deborah number (De) and mobility factor (α) are discussed. Results indicate that entropy generation decreases with increasing De and α while an increase in Br and Br/Ω cause increase in the entropy generation.

Keywords: entropy generation number; Bejan number; annulus; Giesekus constitutive equation; analytical solution.

Reference to this paper should be made as follows: Moayed Mohseni, M. and Rashidi, F. (2015) 'Second law analysis of Giesekus viscoelastic fluid for axial annular flow', *Int. J. Exergy*, Vol. 16, No. 4, pp.404–429.

Biographical notes: Mehdi Moayed Mohseni is a PhD student in the Chemical Engineering Department at Amirkabir University of Technology, Tehran, Iran. He is a teaching assistant for the Fluid Mechanics and Chemical Engineering Thermodynamics courses. His research interests include; non-Newtonian fluid mechanics, heat transfer, computational rheology, transport phenomena, microfluidics and CFD.

Fariborz Rashidi is a Professor of Chemical Engineering at Amirkabir University of Technology, Tehran, Iran. He received his PhD from Chemical Engineering Department of Imperial College of Science and Technology, London, England, in 1982. His main research interests are non-Newtonian flow and heat transfer, rheology and petroleum engineering.

Copyright © 2015 Inderscience Enterprises Ltd.

1 Introduction

Axial flow of non-Newtonian fluids within the annulus are frequently encountered in a wide range of engineering applications such as U-tube heat exchangers in the food-processing industry for heating and cooling of liquid food stuff where the rheological behaviour is generally non-Newtonian and specifically viscoelastic. The rheological behaviour of a drilling mud in oil well drilling industry is thixotropic, shear-thinning and exhibits some degree of viscoelasticity. Extruders play important role in polymer processing and fluids employed in extruders exhibit viscoelastic behaviour. Heat transfer occurs during extrusion process and has major impacts on production rate as well as quality of the final product. Extensive literature exists regarding heat transfer of Newtonian and non-Newtonian fluids in annulus. Shah and London (1978) obtained an analytical solution for forced convection of Newtonian fluid in annular flow without considering viscous dissipation for different boundary conditions. Coelho and Pinho (2006) investigated same problem by including viscous dissipation for the imposed boundary conditions of flux and temperature at the walls. Manglik and Fang (1995) and Fang et al. (1999) studied forced convection for Newtonian and non-Newtonian fluids in the concentric and eccentric annulus using numerical methods without viscous dissipation. Jambal et al. (2005) studied Graetz problem for a power law model fluid and included effects of viscous dissipation and axial conduction. Research on heat transfer of viscoelastic fluid in annulus is rather few. An analytical solution was reported for forced convection heat transfer for fully developed laminar flow of the sPTT viscoelastic model inside a concentric annulus by Hashemabadi et al. (2005). Their study was presented for constant wall heat flux boundary conditions and without considering the effect of viscous dissipation. The same problem was handled more elaborately by Pinho and Coelho (2006).Viscous dissipation effect was included and solutions were presented for both constant heat flux and constant temperature boundary conditions at the walls.

The second law analysis by focusing on entropy generation and its minimisation for systems optimisation has been employed in last several decades. In an engineering system at steady state, the rate of thermodynamic irreversibility ($\dot{\mathrm{I}}$) is equal to the lost useful power or lost work available (Sonntag et al., 2002)

$$\dot{\mathrm{I}} = W_{\mathrm{rev}} - W.$$

The system irreversibility rate is directly proportional to the entropy generation rate and is expressed as below (Sonntag et al., 2002):

$$\dot{\mathrm{I}} = T_0 \, \dot{S}_{\mathrm{gen}}.$$

Thus, any reduction in the rate of entropy generation of a system, e.g., a heat exchanger causes the useful power wasted by the system and consequently the operating cost to decrease. Entropy is generated in all heat transfer systems. There are different sources to cause entropy generation, such as heat transfer across a finite temperature gradient, fluid friction effect, etc. Bejan (1996) investigated different mechanisms causing entropy generation in applied thermal engineering. Entropy generation number and irreversibility distribution ratio in fundamental convective heat transfer were introduced by Bejan (1979) for some example problems. Also Bejan (1982) studied the second law analysis of heat transfer and thermal design and its design-related concept of entropy generation minimisation. Mahmud and Fraser (2002, 2003a) analysed entropy generation and

irreversibility inside an annulus with relative rotation for Newtonian fluid. They obtained analytical solutions for entropy generation and Bejan numbers with isoflux and isothermal boundary conditions. Mahmud and Fraser (2003b) also investigated second law analysis of Newtonian fluid inside channel with circular cross section and two parallel plates by analytical method. The isothermal and isoflux boundary conditions were applied for the study. Also, there exists little investigation concerning entropy generation analysis of power law model fluid. Tasnim and Mahmud (2002a, 2002b) studied the first and second law analysis for Newtonian fluid in a vertical annulus by considering fully developed laminar flow and mixed convection heat transfer, analytically. Mahian et al. (2012) presented first and second laws of thermodynamics to show the effects of MHD flow on distributions of velocity, temperature and entropy generation between two concentric rotating cylinders for Newtonian fluid. The boundary conditions were considered to be different constant temperatures at walls and analytical methods were applied. Mahian et al. (2013a, 2013b) also studied the same problem for fully developed flow and mixed convection with isoflux and isothermal boundary conditions. In isoflux case, for two small deviations around the base radius ratio ($\Pi = 2$), namely $\Pi = 1.9$ and 2.1, the changes in energy cost were calculated. It was found that for $\Pi = 1.9$ energy cost increases by 17.5% while for $\Pi = 2.1$ energy cost is reduced by 13.6%. For non-Newtonian fluid, Yilbas et al. (2004) presented an entropy analysis in annulus by using perturbation approximate method. The flow was considered fully developed and boundary conditions were constant temperatures at the walls. Yurusoy et al. (2004) carried out a similar research by the same method, but viscosity of fluid was assumed to be temperature dependent. Entropy generation in an annular pipe with relative rotation was studied by Kahraman and Yurusoy (2008) for a third-grade fluid. They assumed constant viscosity and isoflux as boundary conditions and calculated velocity and temperature profiles approximately using perturbation method. Mirzazadeh et al. (2008) investigated first and second law analysis in purely tangential flow of non-linear viscoelastic fluid obeying the simplified form of Phan–Thien–Tanner (sPTT) constitutive equation between concentric rotating cylinders. Analytical expressions for dimensionless temperature, entropy generation number and Bejan number were obtained for both isothermal and isoflux boundary conditions.

Although many studies on the first and second law analysis of heat transfer processes have been reported in literature, entropy generation analysis for viscoelastic fluid in axial annular flow has not yet been addressed in literature and the present study might be considered as a first attempt in this context. A modified model with three parameters was suggested by Giesekus (1982) based on molecular ideas in which stresses are considered as non-linear. The privilege of this model is its ability to determine the power law regions for coefficients of viscosity, normal stress and its flexibility to describe elongational viscosity as well as complex viscosity (Bird and Wiest, 1995). This model provides a combination of shear viscosity, shear thinning, non-vanishing normal-stress differences, extensional viscosity with non-exponential stress relaxation and finite asymptotic value and start-up curves. Thus, it could reproduce the major characteristics of polymeric solutions rheology.

The main aim of this study is to present the first and second law analysis for axial annular flow of non-linear viscoelastic fluid obeying Giesekus model in concentric annulus. Two different cases of thermal boundary conditions are considered: uniform heat flux at outer wall and adiabatic inner wall (Case A), and constant temperature at walls (Case B). The governing equations are simplified and analytically solved in the

presence of viscous dissipation. Subsequently, the effects of elasticity, mobility parameter, viscous dissipation and group parameter on dimensionless temperature, entropy generation number and Bejan number are discussed.

2 Governing equation

The annulus is shown schematically in Figure 1. R_i and R_o are inner and outer cylinder radiuses, respectively. The annular gap is defined as $\delta = R_o - R_i$. and κ is the radius ratio (R_i/R_o).

Figure 1 Schematics of an annular duct: (a) cross section; (b) B.Cs for Case A and (c) B.Cs for Case B

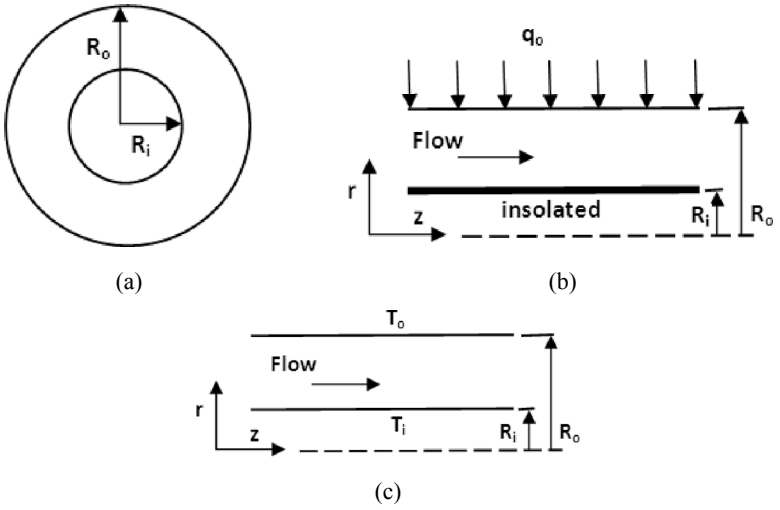

The problem is considered to be steady, laminar and fully developed both thermally and hydrodynamically. The no-slip condition exists at the walls. Axial heat conduction is assumed to be negligible, but the effect of viscous dissipation is included due to high viscosity of viscoelastic fluid and large velocity gradients that exist in industrial flows. It is assumed that temperature variations will not be high enough to impose significant changes in fluid properties and therefore, thermo physical properties of fluid are taken to be constant.

Under these conditions, energy equation for axial flow in the concentric annulus can be represented by the following equation:

$$\rho c_p u \frac{\partial T}{\partial z} = \frac{k}{r}\frac{\partial}{\partial r}\left(r\frac{\partial T}{\partial r}\right) + \Phi, \tag{1}$$

where k, ρ and c_p are thermal conductivity, density and specific heat capacity of the fluid, respectively. T is temperature and Φ is the dissipation function which includes only the shear stress and shear rate for this flow.

$$\Phi = \tau_{zr} \frac{\partial u}{\partial r}. \tag{2}$$

Two different cases of the thermal boundary conditions are considered.

Uniform heat flux at outer wall and adiabatic inner wall (Case A):

$$r = R_i, \quad \frac{\partial T}{\partial r} = 0, \tag{3-a}$$

$$r = R_o, \quad \frac{\partial T}{\partial r} = \frac{q_o}{K}. \tag{3-b}$$

Constant temperatures at the walls (Case B):

$$r = R_i, \quad T = T_i, \tag{4-a}$$

$$r = R_o, \quad T = T_o. \tag{4-b}$$

3 Analytical solution

3.1 Fluid constitutive equation

The Giesekus constitutive equation (without retardation time) is as follows:

$$\tau + \frac{\alpha\lambda}{\eta}(\tau.\tau) + \lambda \frac{\vartheta\tau}{\vartheta t} = 2\eta D, \tag{5}$$

where

$$D = \frac{1}{2}[\nabla u + (\nabla u)^T], \tag{6}$$

$$\frac{\vartheta\tau}{\vartheta t} = \frac{D\tau}{Dt} - [\tau.\nabla u + (\nabla u)^T.\tau], \tag{7}$$

$$\frac{D\tau}{Dt} = \frac{\partial \tau}{\partial t} + (u.\nabla)\tau, \tag{8}$$

where τ is the stress tensor. η and λ are model parameters representing zero shear viscosity and zero shear relaxation time, respectively (Giesekus, 1983). Parameter α in equation (5) is mobility factor that represents anisotropic Brownian motion and/or anisotropic hydrodynamic drag on the constituent polymer molecules (Bird et al., 1987) and it is required that $0 \le \alpha \le 1$ as discussed in Giesekus (1982).

3.2 Hydrodynamic solution

Hydrodynamic solution for this flow was presented by Moayed Mohseni and Rashidi (2010). Equations (9)–(11) are shear rate, shear stress and velocity profile, respectively.

$$\gamma_{rz}^{\circ *} = \frac{1+(2\alpha-1)\mathrm{De}\,\tau_{rr}^*}{\left(1+\mathrm{De}\,\tau_{rr}^*\right)^2}\tau_{rz}^*, \tag{9}$$

$$\tau_{rz}^* = \frac{-\psi R_m^*}{2}\left(\frac{R_m^*}{r}-\frac{r}{R_m^*}\right), \tag{10}$$

$$u^* = V^*\Big|_{R_i^*}^{r^*}, \tag{11}$$

$$V^* = -\frac{1}{4}\psi\,[v_1^* + v_2^* + v_3^*],$$

$$v_1^* = \frac{8(\alpha-1)[A-\mathrm{Br}^{*2}]}{D[AC+DCr^{*4}-2r^{*2}(B+(1-C)^2-2)]},$$

$$v_2^* = \frac{(R_m^{*2}+A(2\alpha-1))\left[\mathrm{Ln}\dfrac{\mathrm{Dr}^{*2}-(1-\sqrt{C})^2}{(1+\sqrt{C})^2-\mathrm{Dr}^{*2}}\right]}{C^{3/2}},$$

$$v_3^* = \frac{(2\alpha-1)}{D\sqrt{C}}\{(1+\sqrt{C})^2\mathrm{Ln}[(1+\sqrt{C})^2-\mathrm{Dr}^{*2}]-\mathrm{Ln}[\mathrm{Dr}^{*2}-(1-\sqrt{C})^2](1-\sqrt{C})^2\};$$

where $A: R_m^{*4}\mathrm{De}^2\alpha\psi^2$, $B: 4+3R_m^{*2}\mathrm{De}^2\alpha\psi^2$, $C: 1+R_m^{*2}\mathrm{De}^2\alpha\psi^2$, $D: \mathrm{De}^2\alpha\psi^2$.

In these equations De is Deborah number, defined as $\mathrm{De}=\lambda U/\delta$ and is related to the level of elasticity, ψ is dimensionless group for pressure gradient and R_m^* refers to radius where the velocity is maximum or $\gamma_{rz}^{\circ *}=0$.

3.3 First law analysis

3.3.1 Solution for uniform wall heat flux boundary conditions (Case A)

For thermally fully developed flow, following relation holds (Bejan, 1995):

$$\frac{\partial}{\partial z}\left(\frac{T_w-T}{T_w-T_b}\right)=0. \tag{12}$$

For the case of constant wall heat flux, equation (12) reduces to:

$$\frac{\partial T}{\partial z}=\frac{\partial T_w}{\partial z}=\frac{\partial T_b}{\partial z}, \tag{13}$$

where T_w and T_b are wall and bulk temperatures, respectively.

Applying energy balance over an infinitesimal element of fluid, dz, the following equation is obtained for fluid bulk temperature gradient in axial direction:

$$\frac{\partial T_b}{\partial z}=\frac{2}{m^{\circ}c_p}\left[q_o R_o+\int_{R_i}^{R_o} r\tau_{zr}\frac{\partial u_z}{\partial r}\mathrm{d}r\right]. \tag{14}$$

By combining equations (1), (13) and (14) and employing dimensionless terms, following equation is obtained:

$$\frac{1}{r^*}\frac{\partial}{\partial r^*}\left(r^*\frac{\partial \Theta}{\partial r^*}\right) = Xu^* - Br\Phi^*, \tag{15}$$

where

$$X = 1 + \frac{2Br\int_{R_i^*}^{R_o^*} r^*\tau^*\frac{\partial u^*}{\partial r^*}\mathrm{d}r^*}{\left(R_o^{*2} - R_i^{*2}\right)}, \tag{16-a}$$

$$\Phi^* = \tau^*\frac{\mathrm{d}u^*}{\mathrm{d}r^*}. \tag{16-b}$$

Mathematical expression for X is presented in the Appendix.

The dimensionless terms are as follows:

$$u^* = \frac{u}{U}, \quad r^* = \frac{r}{\delta}, \quad \tau^* = \frac{\tau}{\eta U/\delta},$$

where U is average velocity over cross-section of the annulus.

We see that Θ is dimensionless temperature and Br is dimensionless Brinkman number which is a measure of importance of viscous dissipation term.

$$\Theta_q = \frac{k\left(T - T_i\right)}{2\delta q^\circ}, \tag{17}$$

$$\mathrm{Br} = \frac{\eta U^2}{2\delta q^\circ}, \tag{18}$$

where

$$q^\circ = \frac{q_o R_o}{R_i + R_o}. \tag{19}$$

Dimensionless thermal boundary conditions will be as follows:

$$\frac{\partial \Theta_q}{\partial r^*} = 0, \quad r^* = R_i^*, \tag{20-a}$$

$$\frac{\partial \Theta_q}{\partial r^*} = \frac{R_i^* + R_o^*}{2R_o^*}, \quad r^* = R_o^*. \tag{20-b}$$

Dimensionless temperature profile (Θ_q) can be obtained by integrating equation (15).

$$\Theta_q = X\bar{U} - \mathrm{Br}\bar{\Phi} + C_1\mathrm{Ln}(r^*) + C_2, \tag{21}$$

$$\bar{U} = \int\frac{1}{r^*}\int u^* r^*\mathrm{d}r^*\mathrm{d}r^*, \tag{22-a}$$

$$\bar{\Phi} = \int \frac{1}{r^*} \int \Phi^* r^* \mathrm{d}r^* \mathrm{d}r^*. \tag{22-b}$$

Mathematical expressions of $\bar{U}$ and $\bar{\Phi}$ are reported in Appendix.

Since both boundary conditions are of second type, determining the value of C_2 is not directly possible. Hence C_2 is eliminated from temperature expression by subtracting dimensionless inner wall temperatures (Θ_{qi}) from dimensionless temperature profile. On the other hand, according to the dimensionless temperature definition (equation (17)), $\Theta_{qi} = 0,$ and therefore Θ_q becomes as shown below:

$$\Theta_q = X\ (\bar{U} - \bar{U}\big|_{R_i^*}) - \mathrm{Br}(\bar{\Phi} - \bar{\Phi}\big|_{R_i^*}) + C_1 \mathrm{Ln}\left(\frac{r^*}{R_i^*}\right), \tag{23}$$

C_1 can be obtained by applying dimensionless boundary conditions (equations (20-a) and (20-b)) as follows:

$$C_1 = R_i \left[\mathrm{Br} \frac{\mathrm{d}\bar{\Phi}}{\mathrm{d}r^*}\bigg|_{r^*=R_i^*} - X \frac{\mathrm{d}\bar{U}}{\mathrm{d}r^*}\bigg|_{r^*=R_i^*} \right] \tag{24-a}$$

or

$$C_1 = R_o \left[\mathrm{Br} \frac{\mathrm{d}\bar{\Phi}}{\mathrm{d}r^*}\bigg|_{r^*=R_o^*} - X \frac{\mathrm{d}\bar{U}}{\mathrm{d}r^*}\bigg|_{r^*=R_o^*} + \frac{R_i^* + R_o^*}{2R_o^*} \right]. \tag{24-b}$$

Mathematical expression of $\mathrm{d}\bar{U}/\mathrm{d}r^*$ and $\mathrm{d}\bar{\Phi}/\mathrm{d}r^*$ are presented in the Appendix.

3.3.2 Solution for constant wall temperature boundary conditions

Dimensionless temperature and Brinkman number are as follows:

$$\Theta_T{}^* = \frac{T - T_i}{T_o - T_i}, \tag{25}$$

$$\mathrm{Br} = \frac{\eta U^2}{K\left(T_o - T_i\right)}. \tag{26}$$

Viscoelastic fluids normally have high viscosity and therefore low Reynolds number such that the advection term $(u\ \partial T/\partial z)$ in energy equation can be neglected. Thus, dimensionless form of energy equation becomes:

$$\frac{1}{r^*} \frac{\partial}{\partial r^*} \left(r^* \frac{\partial \Theta_T^*}{\partial r^*} \right) + \mathrm{Br}\Phi^* = 0 \tag{27}$$

By integrating equation (27), dimensionless temperature profile will be as follows:

$$\Theta_T^* = -\mathrm{Br}\bar{\Phi} + C_3 \mathrm{Ln}(r^*) + C_4. \tag{28}$$

By using the following boundary conditions, C_3 and C_4 can be obtained.

$$\Theta_T^* = 0 \quad \text{at} \quad r^* = R_i^*, \tag{29-a}$$

$$\Theta_T^* = 1 \quad \text{at} \quad r^* = R_o^*, \tag{29-b}$$

$$C_3 = \frac{1 + \mathrm{Br}\left\langle \bar{\Phi}\,|_{r^*=R_o^*} - \bar{\Phi}\,|_{r^*=R_i^*} \right\rangle}{\mathrm{Ln}[R_o^*/R_i^*]}, \tag{30-a}$$

$$C_4 = \frac{\mathrm{Ln}[R_o^*]\bar{\Phi}\,|_{r^*=R_i^*} - \mathrm{Br}\left\langle \bar{\Phi}\,|_{r^*=R_o^*} + 1 \right\rangle \mathrm{Ln}[R_i^*]}{\mathrm{Ln}[R_o^*/R_i^*]}. \tag{30-b}$$

3.4 Second law analysis

According to Bejan (1996), the volumetric rate of entropy generation is defined as

$$\dot{S}_G''' = \frac{k}{T_i^2}(\nabla T)^2 + \frac{\Phi}{T_i}. \tag{31}$$

By substituting Φ from equation (2) into equation (31), $\dot{S}_G'''$ is reduced to following form:

$$\dot{S}_G''' = \frac{k}{T_i^2}\left(\left(\frac{\mathrm{d}T}{\mathrm{d}r}\right)^2 + \left(\frac{\mathrm{d}T}{\mathrm{d}z}\right)^2\right) + \frac{\tau_{zr}}{T_i}\frac{\mathrm{d}u_z}{\mathrm{d}r}. \tag{32}$$

Dimensionless entropy generation rate is called entropy generation number (*Ns*) and it is equal to ratio of volumetric entropy generation to characteristic entropy transfer rate. The characteristic entropy generation rates for two cases of boundary conditions are as follows:

$$\dot{S}_{G,c}''' = \left[\frac{4q^{\circ 2}}{KT_i^2}\right]_{\text{Isoflux}}, \quad \dot{S}_{G,c}''' = \left[\frac{K\left(T_o - T_i\right)^2}{\delta^2 T_i^2}\right]_{\text{Isothermal}}. \tag{33}$$

The axial coordinate is normalised as $z^* = 2z/\delta\,\mathrm{Re}\,\mathrm{Pr}$ with Reynolds and Prandtl numbers defined as $\mathrm{Re} = \rho U 2\delta/\eta$ and $\mathrm{Pr} = \rho c_p/k$, respectively. Also dimensionless temperature for longitudinal temperature gradient $(\mathrm{d}T/\mathrm{d}z)$ is expressed as $\Theta'' = k(T - T_{in})/2\delta q^{\circ}$, where T_{in} represents the inlet temperature. By using characteristic entropy generation rate and dimensionless quantities, equation (32) can be expressed as

$$N_s = \frac{1}{\mathrm{Pe}^2}\left(\frac{\partial\Theta''}{\partial z^*}\right)^2 + \left(\frac{\partial\Theta}{\partial r^*}\right)^2 + \frac{\mathrm{Br}}{\Omega}\tau^*\frac{\mathrm{d}u^*}{\mathrm{d}r^*} = N_C + N_R + N_F. \tag{34}$$

In equation (34), Ω is dimensionless temperature difference which is defined as $\Delta T/T_i$ for isothermal condition and $2q^{\circ}\delta/kT_i$ for isoflux condition. Also ratio Br/Ω is called group parameter, which determines relative importance between viscous dissipation

and heat conduction effects. Pe is Peclet number which determines relative importance between convection and diffusion and for the viscoelastic fluid, it is of order 3000 (Coelho et al., 2002). On the right-hand side of equation (34), the first term (N_C) is entropy generation due to axial conduction heat transfer; second term (N_R) represents entropy generation due to heat transfer in radial direction and the last term (N_F) accounts for entropy generation due to fluid friction. It should be noted that, N_C is inversely proportional to square of Peclet number and since Pe is quite large (≈3000) for viscoelastic fluids, the axial conduction effect (N_C) in entropy generation number (N_s) is negligible (Mahmud and Fraser, 2003b). This has also been reported by Bejan (1979) which reported entropy generation for Pe >> 4 by heat transfer due to axial conduction is negligible.

The contribution of heat transfer and fluid friction can be obtained by using dimensionless temperature, shear stress and velocity profile.

Contributions of heat transfer for two cases of boundary conditions are as follows:

$$N_{RT} = \left(-\mathrm{Br}\frac{\mathrm{d}\bar{\Phi}}{\mathrm{d}r^*} + \frac{1+\mathrm{Br}\left\langle \bar{\Phi}\big|_{r^*=R_o^*} - \bar{\Phi}\big|_{r^*=R_i^*} \right\rangle}{r\mathrm{Ln}[R_o^*/R_i^*]} \right)^2, \tag{35}$$

$$N_{Rq} = \left(X\left\langle \frac{\mathrm{d}\bar{U}}{\mathrm{d}r^*} - \frac{R_i}{r}\frac{\mathrm{d}\bar{U}}{\mathrm{d}r^*}\Big|_{r^*=R_i^*} \right\rangle - \mathrm{Br}\left\langle \frac{\mathrm{d}\bar{\Phi}}{\mathrm{d}r^*} - \frac{R_i}{r}\frac{\mathrm{d}\bar{\Phi}}{\mathrm{d}r^*}\Big|_{r^*=R_i^*} \right\rangle \right)^2. \tag{36}$$

Since flow and thermal fields are independent, fluid friction contributions would be similar for both isothermal and isoflux boundary conditions.

$$N_F = \frac{\mathrm{Br}}{\Omega}\frac{R_m^{*2}\left(\frac{R_m^*}{r^*}-\frac{r^*}{R_m^*}\right)^2\psi^2\left(1-\frac{1}{4}R_m^{*2}\mathrm{De}^2\left(\frac{R_m^*}{r^*}-\frac{r^*}{R_m^*}\right)^2\alpha(2\alpha-1)\psi^2\right)}{4\left(1-\frac{1}{4}R_m^{*2}\mathrm{De}^2\left(\frac{R_m^*}{r^*}-\frac{r^*}{R_m^*}\right)^2\alpha\psi^2\right)^2}. \tag{37}$$

3.5 Fluid vs. heat transfer irreversibility

To investigate irreversibility distribution, Bejan number (Be) which is ratio of entropy generation due to heat transfer to total entropy generation (Paoletti et al., 1989), could be defined as

$$\mathrm{Be} = \frac{N_R}{N_R + N_F}. \tag{38}$$

It is clear that Bejan number varies from 0 to 1. When Be = 0, entropy generation will be dominated by fluid friction effects and for Be = 1 entropy generation is dominated by heat transfer. For Be = 1/2, heat transfer and fluid friction have equal contribution to the entropy generation.

3.6 Global entropy generation

The volumetric average entropy generation rate ($[N_s]_{av}$) is defined as follows:

$$[N_S]_{\text{ave}} = \frac{1}{\forall}\int N_S \, \mathrm{d}\forall = \frac{1}{\forall}\int N_S r \, \mathrm{d}\theta \, \mathrm{d}r \, \mathrm{d}z. \tag{39}$$

Dimensionless form of equation (39) is as below:

$$[N_S]_{\text{ave}} = \frac{2}{R_o^{*2} - R_i^{*2}}\int_{R_i^*}^{R_o^*} N_S \, r \, \mathrm{d}r. \tag{40}$$

By substituting entropy generation number (N_s) into equation (40), the average entropy generation rate could be obtained. However, due to the complexity of integration process, handling of this integral does not seem to be possible analytically. Thus, commercial software based on Gauss–Kronrod numerical method was employed for determining this value.

3.7 Validation

If α and De in the Giesekus equation are set as zero the model will become Newtonian. Therefore, it is expected that by choosing very small values for α and De, the results obtained for viscoelastic fluid to be similar to those of Newtonian fluid. This way, one can verify the accuracy of obtained equations for viscoelastic fluid.

Equations (16-a), (22-a), (22-b), (36) and (37) for Newtonian fluid are derived as follows:

$$\begin{aligned} X &= 1 + \frac{2\mathrm{Br}\int_{R_i^*}^{R_o^*} r^* \left(\frac{\partial u^*}{\partial r^*}\right)^2 \mathrm{d}r^*}{\left(R_o^{*2} - R_i^{*2}\right)} \\ &= 1 - \frac{1}{8}\frac{\mathrm{Br}\,\psi^2\left(\left(R_i^{*2} - R_o^{*2}\right)\left(R_i^{*2} - 4R_m^{*2} + R_o^{*2}\right) + 4R_m^{*2}\mathrm{Ln}\left(\frac{R_i^*}{R_o^*}\right)\right)}{\left(R_o^{*2} - R_i^{*2}\right)}, \end{aligned} \tag{41}$$

$$\bar{U} = \int \frac{1}{r^*}\int u^* r^* \mathrm{d}r^* \mathrm{d}r^* = \frac{1}{64} r^{*2}\psi\left(r^{*2} - 4R_i^{*2} + 8R_m^{*2} - 8R_m^{*2}\mathrm{Ln}\left(\frac{r^*}{R_i^*}\right)\right), \tag{42-a}$$

$$\bar{\Phi} = \int \frac{1}{r^*}\int \Phi^* r^* \mathrm{d}r^* \mathrm{d}r^* = \frac{1}{64}\psi\left(r^{*4} - 8r^{*2}R_m^{*2} + 8R_m^{*4}\mathrm{Ln}^2(r^*)\right), \tag{42-b}$$

$$N_{Rq} = \frac{\psi\left(\begin{array}{l}\left(r^{*2}-R_i^{*2}\right)\left(r^{*2}-R_i^{*2}+2R_m^{*2}\right)\\ -4r^{*2}R_m^{*2}\mathrm{Ln}\left(\dfrac{r^*}{R_i^*}\right)\end{array}\right)\left(1-\dfrac{1}{8}\dfrac{\mathrm{Br}\psi^2\left(\begin{array}{l}\left(R_i^{*2}-R_o^{*2}\right)\left(R_i^{*2}-4R_m^{*2}+R_o^{*2}\right)\\ +4R_m^{*2}\mathrm{Ln}\left(\dfrac{R_i^*}{R_o^*}\right)\end{array}\right)}{\left(R_o^{*2}-R_i^{*2}\right)}\right)}{16r^*},$$
$$-\frac{\mathrm{Br}\psi^2\left(\left(r^{*2}-R_i^{*2}\right)\left(r^{*2}+R_i^{*2}-4R_m^{*2}\right)+4R_m^{*4}\mathrm{Ln}\left(\dfrac{r^*}{R_i^*}\right)\right)}{16r^*} \tag{43}$$

$$N_F = \frac{\mathrm{Br}}{\Omega}R_m^{*2}\left(\frac{R_m^*}{r^*}-\frac{r^*}{R_m^*}\right)^2\psi^2. \tag{44}$$

Table 1 compares N_{sq} and Be_q with various r values for Newtonian fluid and viscoelastic fluid with $\alpha = 0.05$ and De = 0.01. Results confirm the accuracy of obtained equations for the Giesekus model employed in this study.

Table 1 Comparison of N_{sq} and Be_q for Newtonian and viscoelastic fluids at Br/Ω = 1, Br = 1

$r^* =$	*1*	*1.2*	*1.4*	*1.6*	*1.8*	*2*
N_{sq} (Newtonian)	48.0208	26.0367	1.6472	9.2008	28.2869	30.4271
N_{sq} ($\alpha = 0.05$ De = 0.01)	48.0205	26.0214	1.6451	9.1969	28.2752	30.4222
Be_q (Newtonian)	0	0.50447	0.54299	0.76410	0.55233	0.01848
Be_q ($\alpha = 0.05$ De = 0.01)	0	0.50445	0.54286	0.76410	0.55232	0.01849

4 Results and discussions

Figure 2 presents effects of Deborah and Brinkman numbers on dimensionless temperature distribution for both isoflux and isothermal boundary conditions. For large Deborah numbers, fluid is heated up with a uniform slope from colder wall to the warmer wall. However, for smaller Deborah numbers temperature profiles show a maximum value within the annular gap. Increasing Brinkman and decreasing Deborah have the same effect on temperature profile. In other words, increasing both Brinkman and Deborah have opposite effects on temperature profile, because by increasing Brinkman the internally generated heat by viscous dissipation increases, but when Deborah increases due to shear-thinning behaviour of fluid, internally generated heat decreases. In the case of isoflux (Figure 2(a)), internal heat generation by viscous dissipation

at large Brinkman or small Deborah is stronger near the walls and is expected; because according to viscous dissipation function (equation (2)), both shear stress and velocity gradient attain their maximum values adjacent to the walls. Therefore, the difference between annular fluid temperature and wall temperature increases by increasing Brinkman or decreasing Deborah and the temperature profiles show a maximum.

Figure 2 Dimensionless temperature profile with variation De for $\alpha = 0.1$, Br = 0.01 (no symbols) and Br = 1 (O): (a) isoflux case and (b) isothermal case

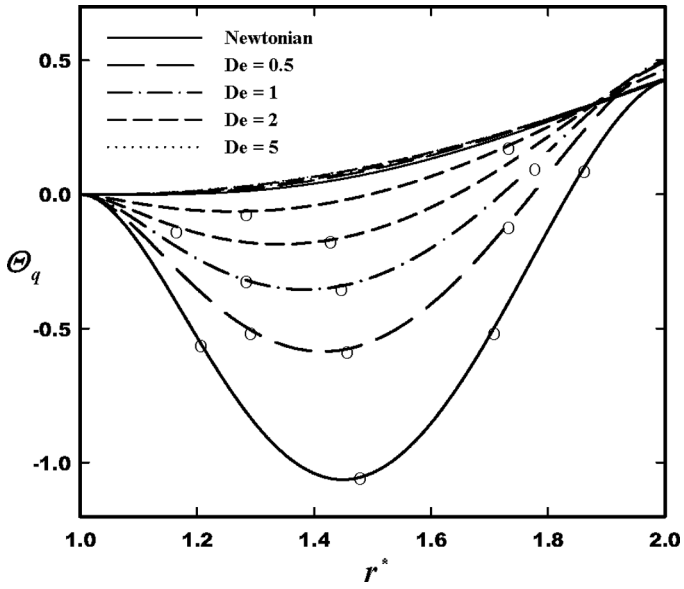

(a)

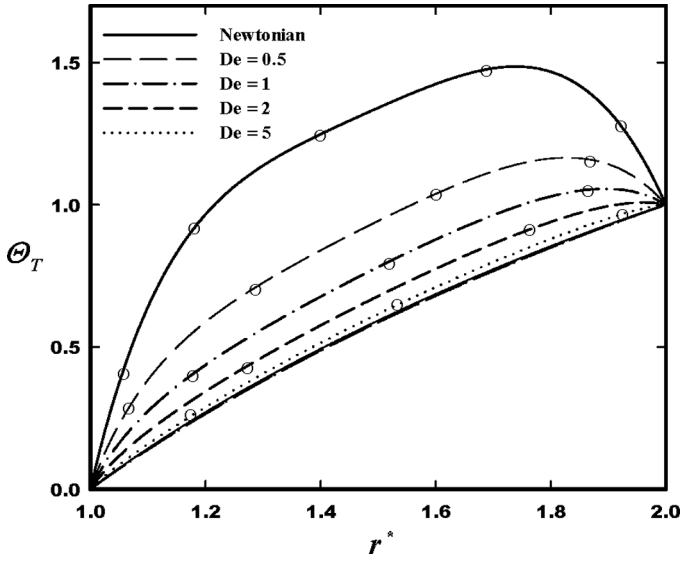

(b)

Maximum point in Figure 2(b) is due to the magnitude of internally generated heat. This value rises by increasing Brinkman or decreasing Deborah and causes higher fluid temperatures but since the boundary conditions are constant temperatures at the walls, the fluid temperature would eventually become higher than the warmer wall temperature and a maximum temperature will occur near the warmer wall. The maximum point is important because entropy generation due to heat transfer is zero (Be = 0) at this point.

Figure 3 shows effect of group parameter (Br/Ω) on entropy generation numbers (N_{ST}, N_{Sq}). As can be seen from Figure 3(a) and (b), entropy generation number increases by increasing group parameter because by increasing Br/Ω , entropy generation rate due to fluid friction (N_F) increases (see equation (34)).

Entropy generation reaches high values in regions close to the walls and becomes more pronounced towards the inner wall. This is because maximum viscous dissipation occurs in this region. When Br/Ω = 0, the effect of fluid friction contribution (N_F) is removed from entropy generation rate and it only becomes influenced by heat transfer contribution (N_R). For this reason N_{Sq} becomes zero at inner wall (see Figure 3(b)) because inner wall temperature gradient is zero for isoflux conditions (see Figure 2(a)).

Effect of Brinkman number on entropy generation number is shown in Figure 4. Parameters α, De and Br/Ω are assumed constant. As a result, for any specified radial location in annulus N_F will be unchanged and only variations of N_R will change entropy generation number. It is seen that increasing Brinkman number increases entropy generation number for both isoflux and isothermal cases because increasing Brinkman number increases temperature gradient (see Figure 2). For isothermal conditions (Figure 4(a)), entropy generation profiles coincide in central region of the annulus. This is because temperature gradients in central region are almost equal for different Brinkman numbers (see Figure 2(b)).

Figure 3 Effect of group parameter on the entropy generation for Br = 1, De = 1 and α = 0.1: (a) isothermal case and (b) isoflux case

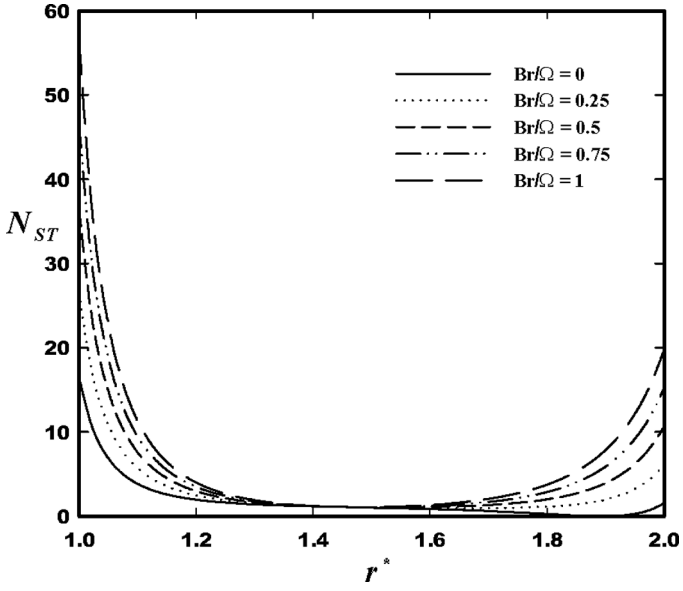

(a)

Figure 3 Effect of group parameter on the entropy generation for Br = 1, De = 1 and $\alpha = 0.1$: (a) isothermal case and (b) isoflux case (continued)

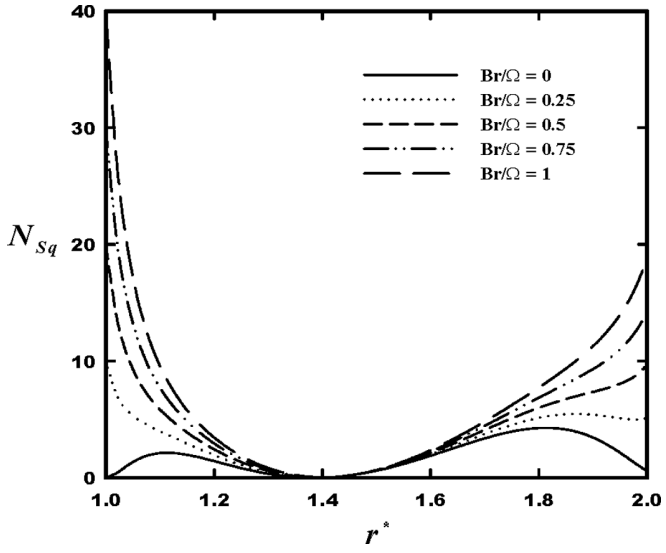

(b)

Figure 5 shows effect of Deborah number on entropy generation number for isothermal case. Drop in N_{ST} by increasing fluid elasticity is due to shear thinning behaviour of the Giesekus fluid. Increase in elasticity causes temperature gradient and viscose dissipation effect to decrease. Therefore, entropy generation decreases.

Figure 4 Effect of Brinkman number on the entropy generation for Br/Ω = 1, De = 1 and $\alpha = 0.1$: (a) isothermal case and (b) isoflux case

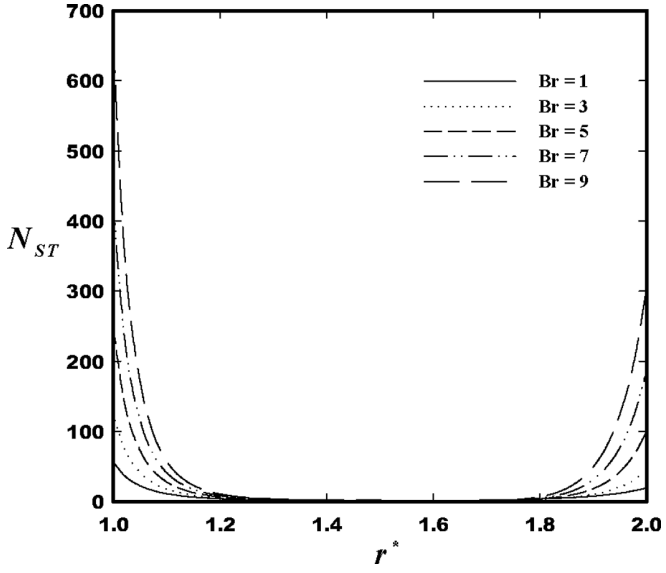

(a)

Figure 4 Effect of Brinkman number on the entropy generation for Br/Ω = 1, De = 1 and $\alpha = 0.1$: (a) isothermal case and (b) isoflux case (continued)

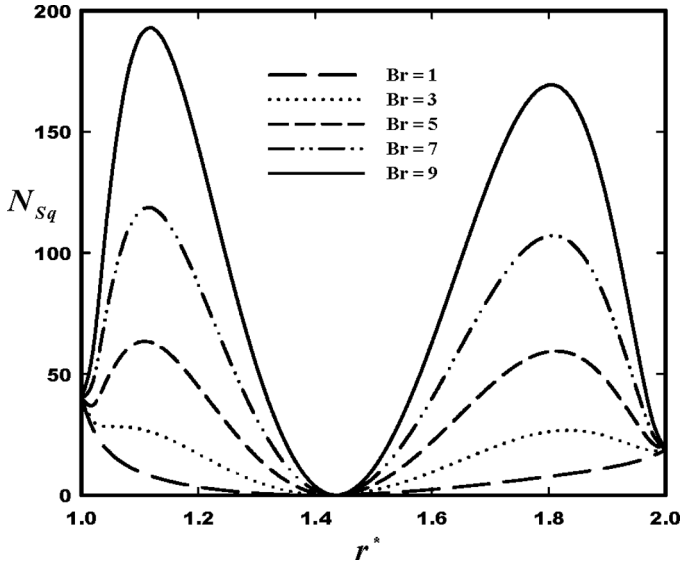

(b)

Figure 5 Effect of Deborah number on the isothermal entropy generation for Br/Ω = 1, Br = 5 and $\alpha = 0.1$

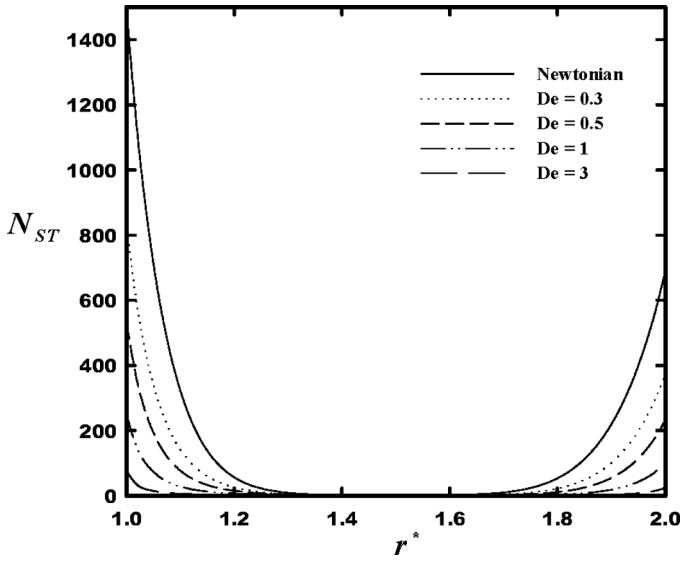

Figure 6 presents effect of mobility factor on entropy generation number for isoflux case. Influence of mobility factor is similar to the effect of Deborah number because mobility factor can indirectly be related to concentration of polymer, e.g., $\alpha = 0$ represents dilute solutions, while $\alpha = 0.5$ represents highly concentrated solutions (Bhatar et al., 2005). Hence, elasticity is directly related to mobility factor.

Figure 6 Effect of mobility factor on the isoflux entropy generation for Br/Ω = 1, Br = 5 and De = 1

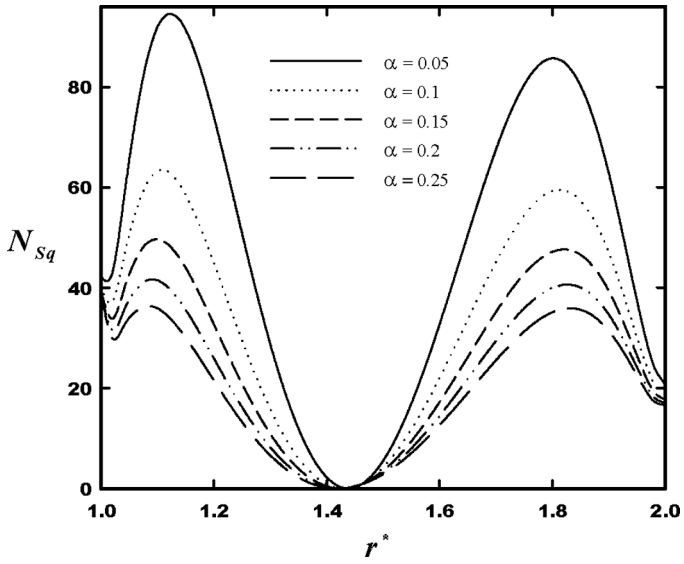

Figure 7 shows effect of group parameter on Bejan number (Be_T). As it is shown in this figure for Br/Ω = 0, Bejan number is at its maximum value ($Be_T = 1$), which indicates that there is no contribution of fluid friction to entropy generation. As Br/Ω increases, Bejan number decreases that implies rise in the fluid friction contribution to entropy generation. Also for all values of group parameter, Bejan number profiles exhibit a maximum and a minimum within the annular gap which are 1 and 0, respectively. The radial locations of extreme points are independent of group parameter values. The minimum point in Bejan numbers is due to existence of the maximum point in temperature profile which implies zero temperature gradient ($\partial\Theta_T/\partial r^* = 0$) and consequently N_R and Be_T both become zero. This minimum point occurs at $r^*_{\min} \approx 1.895$ in Bejan profile for all values of group parameter. The radial location of maximum point in Bejan profile is always at $r^*_{\max} \approx 1.445$. This point is in fact R^*_m which refers to the radius where shear stress is zero and consequently dissipation function becomes zero (see equation (2)). Therefore, at this point fluid friction contribution (N_F) is removed from total entropy generation and subsequently Be_T becomes equal to 1.

Effect of Brinkman number on Be_T is shown in Figure 8. Maximum point in Bejan profile ($Be_T = 1$) is similar to Figure 7 which occurs at $R^*_m = 1.445$ for all values of Brinkman number because this point is related to flow field and is independent of thermal parameters. But, it is seen that minimum point ($Be_T = 0$), i.e., where $\partial\Theta_T/\partial r^* = 0$, in Bejan profile is not fixed and for smaller values of *Br* it shifts towards the outer wall. Also Bejan profiles intersect each other in the neighbourhood of $r^* = 1.663$, where contribution of heat transfer to entropy generation is similar for all Brinkman numbers.

Bejan number (Be_T) is plotted in Figure 9 as a function of radial distance for different values of Deborah number. In this case, locations of minimum and maximum points vary with different values of Deborah number because elasticity level of fluid influences both flow and thermal fields. Fluid friction as well as heat transfer contribution to entropy generation decrease from inner wall to R^*_m in a manner which makes Bejan number to

rise. But as can be seen from the figure, for Newtonian fluid profile unlike the other profiles, Bejan number reduces from the inner wall until it reaches to $r^* = 1.267$ which means that fluid friction contribution to entropy generation increases. This is because decrease of temperature gradient in Newtonian fluid is quickly than viscous dissipation decrease in this region (see Figure 2(b)) which implies that ratio of numerator to denominator of Bejan fraction is being reduced.

Figure 7 Effect of group parameter on the isothermal Bejan number for Br = 1, De = 1 and $\alpha = 0.1$

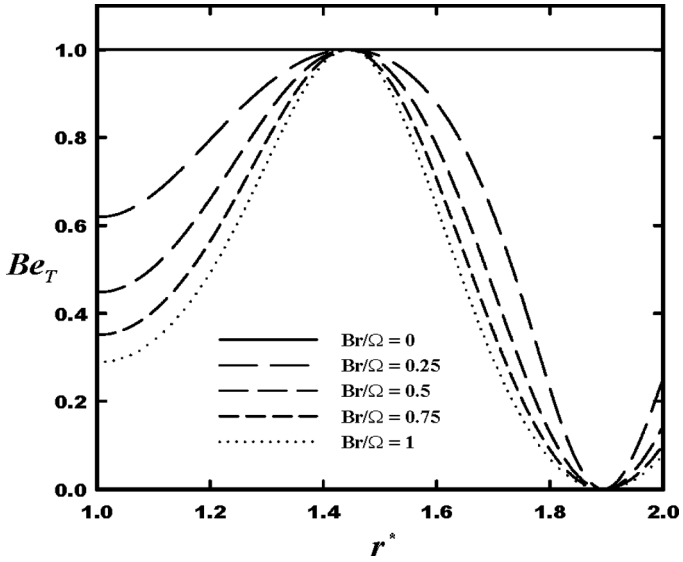

Figure 8 Effect of Brinkman number on the isothermal Bejan number for Br/Ω = 1, De = 1 and $\alpha = 0.1$

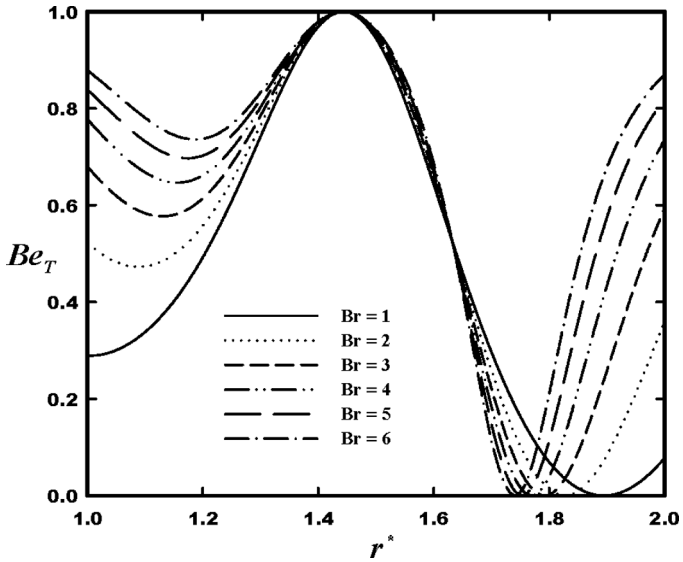

Figure 9 Effect of Deborah number on the isothermal Bejan number for Br/Ω = 1, Br = 1 and $\alpha = 0.1$

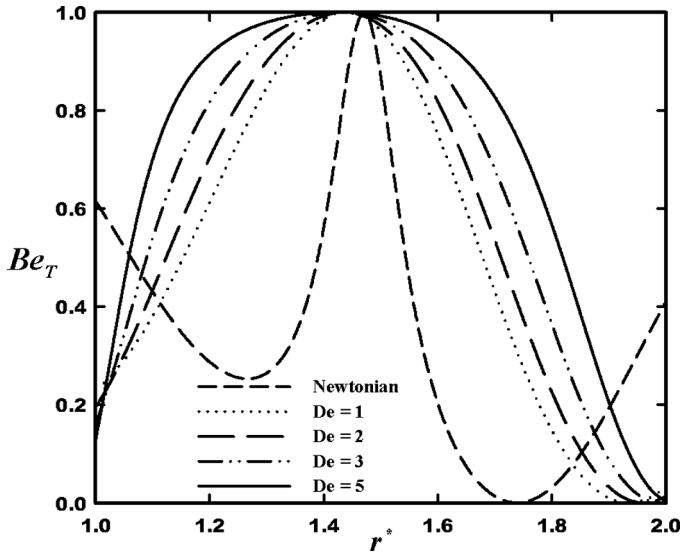

Figure 10 shows effects of group parameter and Brinkman number on average entropy generation for isothermal case ($[N_{ST}]_{ave}$). It is seen that $[N_{ST}]_{ave}$ increases by increasing Br/Ω and Br. Because by increasing Br/Ω, entropy generation rate due to fluid friction (N_F) rises and by increasing Brinkman number heat transfer contribution to entropy generation (N_R) increases.

Figure 10 Variation of average entropy generation for isothermal case vs. the Br and different values of Br/Ω at $\alpha = 0.1$ and De = 1

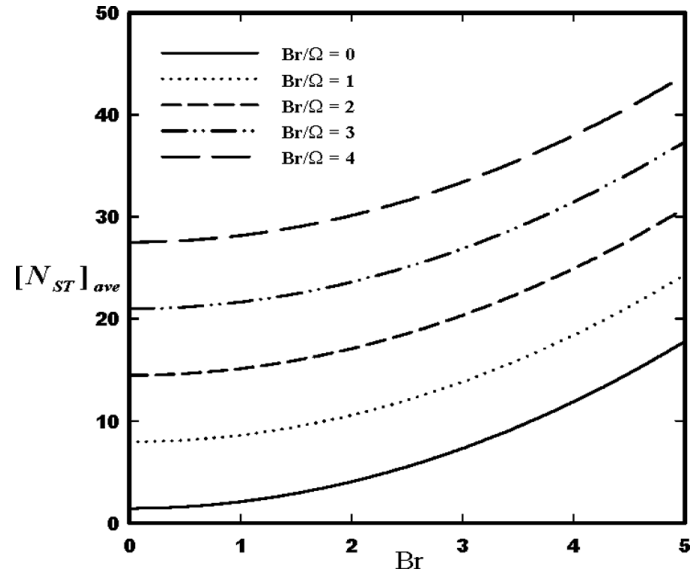

Figure 11 shows distribution of $[N_{ST}]_{ave}$ as function of Deborah number at different mobility factors which is again related to the shear thinning behaviour of fluid where by increasing fluid elasticity, contribution of fluid friction as well as heat transfer to entropy generation decreases. Also, in comparison with Newtonian fluid the magnitude of average entropy generation rate decreases more than 50% when Deborah number approaches 0.5.

Figure 11 Variation of average entropy generation for isothermal case vs. the De and different values of α at Br/Ω = 1 and Br = 1

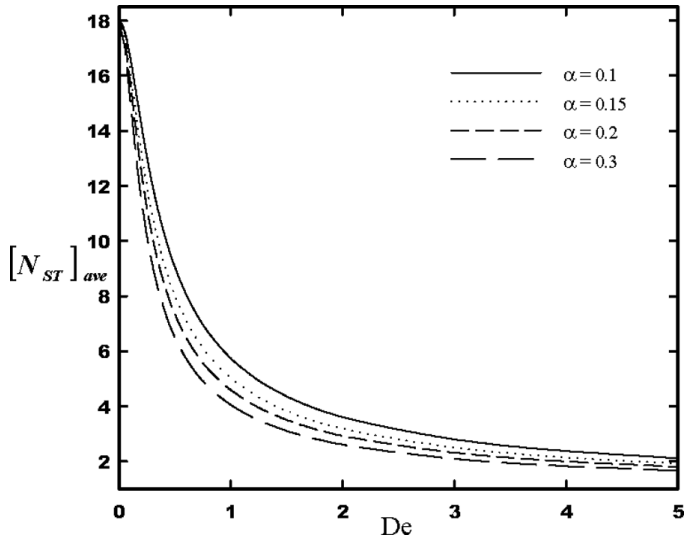

5 Conclusions

First and second laws of thermodynamics have been analytically investigated for axial annular flow of non-linear viscoelastic fluid obeying the Giesekus constitutive equation. It was concluded that, for low Brinkman numbers or large Deborah numbers temperature profile has a uniform slope, but by increasing Brinkman or decreasing Deborah temperature profiles show a maximum. The entropy generation number (N_S) rises by increasing group parameter (Br/Ω) and Brinkman number (Br) but decreases by increasing Deborah number (De) and mobility factor (α). Also, high values of Entropy generation occur at inner wall. All Bejan number profiles show a minimum point (Be = 0) and a maximum point (Be = 1) inside the annular gap. The minimum point occurs due to existence of a peak in temperature distribution ($\partial\Theta_T/\partial r^* = 0$). The maximum point is due to disappearance of viscous dissipation effect and its location is always at R^*_m. The maximum and minimum values of Bejan number indicate that entropy generation is dominated only by heat transfer and fluid friction, respectively. Magnitude of average entropy generation rate decreases more than 50% when Deborah number approaches 0.5.

References

Bejan, A. (1979) 'A study of entropy generation in fundamental convective heat transfer', *Journal of Heat Transfer*, Vol. 101, No. 4, pp.718–725.

Bejan, A. (1982) 'Second-law analysis in heat transfer and thermal design', *Advances in Heat Transfer*, Vol. 15, pp.1–58.

Bejan, A. (1995) *Convection Heat Transfer*, Wiley, New York.

Bejan, A. (1996) *Entropy Generation Minimization*, CRC, Boca Raton, NY.

Bhatar, G., Shaqfeh, E.S.G. and Khomami, B. (2005) 'The influence of polymer concentration and chain architecture on free surface displacement flows of polymeric fluids', *Journal of Rheology*, Vol. 49, No. 5, pp.929–963.

Bird, R.B. and Wiest, J.M. (1995) 'Constitutive equations for polymeric liquids', *Annual Review of Fluid Mechanics*, Vol. 27, pp.169–193.

Bird, R.B., Armstrong, R.C. and Hassager, O. (1987) 'Dynamics of polymeric liquids', *Fluid Dynamics*, Vol. 1, 2nd ed., Wiley, New York.

Coelho, P.M. and Pinho, F.T. (2006) 'Fully-developed heat transfer in annuli with viscous dissipation', *International Journal of Heat and Mass Transfer*, Vol. 49, Nos. 19–20, pp.3349–3359.

Coelho, P.M., Pinho, F.T. and Oliveira, P.J. (2002) 'Fully developed forced convection of the Phan-Thien–Tanner fluid in ducts with a constant wall temperature', *International Journal of Heat Mass Transfer*, Vol. 45, No. 7, pp.1413–1423.

Fang, P., Manglik, R.M. and Jog, M.A. (1999) 'Characteristics of laminar viscous shear thinning fluid flows in eccentric annular channels', *Journal of Non-Newtonian Fluid Mechanics*, Vol. 84, No. 1, pp.1–17.

Giesekus, H. (1982) 'A simple constitutive equation for polymer fluids based on the concept of deformation-dependent tensorial mobility', *Journal of Non-Newtonian Fluid Mechanics*, Vol. 11, Nos. 1–2, pp.69–109.

Giesekus, H. (1983) 'Stressing behaviour in simple shear flow as predicted by a new constitutive model for polymer fluids', *Journal of Non-Newtonian Fluid Mechanics*, Vol. 12, No. 3, pp.367–374.

Hashemabadi, S.H., Etemad, S.Gh. and Thibault, J. (2005) 'Analytical solution of viscoelastic fluid flow and heat transfer through an annulus', *Heat Transfer Engineering*, Vol. 26, No. 2, pp.45–49.

Jambal, O., Shigechi, T., Davaa, G. and Momoki, S. (2005) 'Effects of viscous dissipation and fluid axial heat conduction on heat transfer for non-Newtonian fluids in ducts with uniform wall temperature. Part II: Annular ducts', *International Communications in Heat and Mass Transfer*, Vol. 32, No. 9, pp.1174–1183.

Kahraman, A. and Yurusoy, M. (2008) 'Entropy generation due to non-Newtonian fluid flow in annular pipe with relative rotation: constant viscosity case', *Journal of Theoretical and Applied Mechanics*, Vol. 46, No. 1, pp.69–83.

Mahian, O., Mahmud, S. and Pop, I. (2012) 'Analysis of first and second laws of thermodynamics between two isothermal cylinders with relative rotation in the presence of MHD flow', *International Journal of Heat and Mass Transfer*, Vol. 55, Nos. 17–18, pp.4808–4816.

Mahian, O., Oztop, H., Pop, I., Mahmud, S. and Wongwises, S. (2013a) 'Entropy generation between two vertical cylinders in the presence of MHD flow subjected to constant wall temperature', *International Communications in Heat and Mass Transfer*, Vol. 44, pp.87–92.

Mahian, O., Oztop, H., Pop, I., Mahmud, S. and Wongwises, S. (2013b) 'Design of a vertical annulus with MHD flow using entropy generation analysis', *Thermal Science*, Vol. 17, No. 4, pp.1013–1022.

Mahmud, S. and Fraser, R.A. (2002) 'Second law analysis of heat transfer and fluid flow inside a cylindrical annular space', *International Journal of Exergy*, Vol. 2, No. 4, pp.322–329.

Mahmud, S. and Fraser, R.A. (2003a) 'Analysis of entropy generation inside cylindrical annuli with relative rotation', *International Journal of Thermal Sciences*, Vol. 42, No. 5, pp.513–521.

Mahmud, S. and Fraser, R.A. (2003b) 'The second law analysis in fundamental convective heat transfer problems', *International Journal of Thermal Sciences*, Vol. 42, No. 2, pp.177–186.

Manglik, R.M. and Fang, P. (1995) 'Effect of eccentricity and thermal boundary conditions on laminar flow in annular ducts', *International Journal of Heat Fluid Flow*, Vol. 16, No. 4, pp.298–306.

Mirzazadeh, M., Shafaei, A. and Rashidi, F. (2008) 'Entropy analysis for non-linear viscoelastic fluid in concentric rotating cylinders', *International Journal of Thermal Sciences*, Vol. 47, No. 12, pp.1701–1711.

Moayed Mohseni, M. and Rashidi, F. (2010) 'Viscoelastic fluid behaviour in annulus using Giesekus model', *Journal of Non Newtonian Fluid Mechanics*, Vol. 165, Nos. 21–22, pp.1550–1553.

Paoletti, S., Rispoli, F. and Sciubba, E. (1989) 'Calculation of exergetic losses in compact heat exchanger passages', *ASME AES*, Vol. 10, No. 2, pp.21–29.

Pinho, F.T. and Coelho, P.M. (2006) 'Fully-developed heat transfer in annuli for viscoelastic fluids with viscous dissipation', *Journal of Non-Newtonian Fluid Mechanics*, Vol. 138, No. 1, pp.7–21.

Shah, R.K. and London, A.L. (1978) *Laminar Flow Forced Convection in Ducts*, Academic Press, New York.

Sonntag, R.E., Borgnakke, C. and Van Wylen, G.J. (2002) *Fundamentals of Thermodynamics*, Wiley, New York.

Tasnim, S.H. and Mahmud, S. (2002a) 'Mixed convection and entropy generation in a vertical annular space', *International Journal of Exergy*, Vol. 2, No. 4, pp.373–379.

Tasnim, S.H. and Mahmud, S. (2002b) 'Entropy generation in a vertical concentric channel with temperature dependent viscosity', *International Communications in Heat and Mass Transfer*, Vol. 29, No. 7, pp.907–918.

Yilbas, B.S., Yurusoy, M. and Pakdemirli, M. (2004) 'Entropy analysis for non-Newtonian fluid flow in annular pipe: constant viscosity case', *Entropy*, Vol. 6, No. 3, pp.304–315.

Yurusoy, M., Yilbas, B.S. and Pakdemirli, M. (2004) 'Non-Newtonian fluid flow in annular pipes and entropy generation: temperature-dependent viscosity', *Sadhana*, Vol. 31, No. 6, pp.683–695.

Nomenclature

Be	Bejan number
Br	Brinkman number
C	Integration constant
c_p	Specific heat at constant pressure, J/kg.K
De	Deborah number, De = $\lambda U/\delta$
k	Thermal conductivity, Watt/m.K
N_C	Entropy generation number; axial conduction contribution
N_F	Entropy generation number; fluid friction contribution
N_R	Entropy generation number; radial heat transfer contribution
N_S	Entropy generation number; total

Pr	Prandtl number, $\rho c_p/k$
q	Heat flux, Watt/m^2
r	Radial coordinate, m
R_i	Radius of inner cylinder
R_o	Radius of outer cylinder
R_m	Radius where velocity is maximum
Re	Reynolds number, $\rho U2\delta/\eta$
$\dot{S}'''_G$	Entropy generation rate, Watt/m^3.K
$\dot{S}'''_{G,c}$	Characteristic entropy generation rate
t	Time, s
T	Fluid temperature, K
u	Velocity, m/s
U	Average velocity
z	Axial coordinate, m
Greek symbols	
α	Mobility factor
δ	Annular gap, $\delta = R_o - R_i$
$\dot{\gamma}$	Shear rate tensor, s^{-1}
η	Zero-shear viscosity, Pa.s
λ	Zero-shear relaxation time, s
ρ	Fluid density, kg/m^3
τ	Stress tensor, Pa
ψ	Dimensionless group for pressure gradient
κ	Radius ratio
Ω	Dimensionless temperature difference
Φ	Viscous dissipation function
θ	Tangential coordinate
Θ	Dimensionless temperature for isoflux boundary conditions
ϑ	Convected derivative
$\forall$	Volume of the annular gap (m^3)
Subscripts	
ave	Average value
b	Bulk value
in	Inlet
i	Inner wall
o	Outer wall

q	Isoflux boundary condition
T	Isothermal boundary condition
w	Wall value
Superscripts	
*	Refers to dimensionless quantities
T	Transpose of tensor

Appendix

$$a = 1 + C + 2\sqrt{C} \quad \bar{a} = -1 - C + 2\sqrt{C} \quad m = 1 + 2C - C^2 \quad H = \frac{D}{\psi}$$

$$F_1 = \frac{R_m^{*2} + A(2\alpha - 1)}{C\sqrt{C}} \quad F_2 = \frac{2\alpha - 1}{D\sqrt{C}} \quad F_3 = aF_2 - F_1 \quad \bar{F}_3 = \bar{a}F_2 + F_1$$

$$F_4 = \sqrt{1 + B^2 + 4C - 4C^3 + C^4 - 2Bm + 2C^2 - C^2 AD} \quad F_5 = 1 - B + 2C - C^2$$

$$F_6 = -\frac{4\left(B^2 - ACD + B(-m + F_4)\right)(\alpha - 1)}{CD^2 F_4} \quad \bar{F}_6 = \frac{4\left(B^2 - ACD - B(m + F_4)\right)(\alpha - 1)}{CD^2 F_4}$$

$$F_7 = -\frac{aF_3}{D} \quad \bar{F}_7 = \frac{\bar{a}\bar{F}_3}{D} \quad F_8 = D\left(AC + R_i^{*2}(2 - 2B + 4C - 2C^2 + CDR_i^{*2})\right)$$

$$F_9 = 8(1 - \alpha)(BR_i^{*2} - A) + 8DF_2 R_i^{*2}\sqrt{C}\,F_5 + 4C\sqrt{C}DF_2(A + DR_i^{*4})$$

$$F_{10} = ACDF_1 + 2DF_1 R_i^{*2} F_5 + D^2 F_1 R_i^{*4} C$$

$$F_{11} = 0.5\left(F_1 - \bar{F}_3 - \frac{F_{10}}{F_8} - \frac{F_9}{F_8} - F_3 - \frac{F_{10}}{F_8}\mathrm{Ln}\left(\frac{\bar{a} + \mathrm{DR}_i^{*2}}{a - \mathrm{DR}_i^{*2}}\right)\right) \quad F_{12} = \frac{0.5a}{D}\left(F_1 - \frac{F_{10}}{F_8} - F_3\right)$$

$$F_{13} = F_7\,\mathrm{Ln}|a| + \bar{F}_7\,\mathrm{Ln}|\bar{a}| + F_6\,\mathrm{Ln}|F_4 - F_5| + \bar{F}_6\,\mathrm{Ln}|F_4 + F_5| \quad F_{14} = \frac{1}{2}\left(\frac{F_{10}}{F_8} + F_3\right)$$

$$F_{15} = 0.5\,(\bar{F}_3 - F_1)$$

$$F_{16} = 1 + C^2 - R_m^{*4} D^2 \quad F_{17} = \sqrt{1 + 2C + C^2 - R_m^{*4} D^2} \quad F_{18} = \frac{R_m^{*4}(\alpha - 1)\psi^2}{C\sqrt{C}}$$

$$F_{19} = \frac{4\alpha - 3}{H^2\sqrt{C}} \quad F_{20} = \frac{1 - 2\alpha}{2\alpha\,\mathrm{De}^2} \quad F_{21} = \frac{4(1 + C)(\alpha - 1)}{CH^2}$$

$$F_{22} = \frac{(F_{17} - F_{16} + C(6 + F_{17}))(\alpha - 1)}{CH^2 F_{17}} \quad \bar{F}_{22} = \frac{(F_{17} + F_{16} + C(-6 + F_{17}))(\alpha - 1)}{CH^2 F_{17}}$$

$$F_{23} = 1 + C + F_{17} \quad \bar{F}_{23} = -1 - C + F_{17} \quad F_{24} = -4R_m^{*4} D\,(1 + C)\,(\alpha - 1)$$

Appendix (continued)

$$F_{25} = 4\,(8C + R_m^{*4} D^2)\;(\alpha - 1) \quad F_{26} = F_{18} - a\,F_{19} \quad \overline{F}_{26} = F_{18} + \overline{a}\,F_{19}$$

$$F_{27} = R_m^{*4} D - 2\,(1 + C)\,R_o^{*2} + R_o^{*4} D \quad \overline{F}_{27} = R_m^{*4} D - 2\,(1 + C)\,R_i^{*2} + R_i^{*4} D$$

$$F_{28} = F_{20}\,(R_o^{*2} - R_i^{*2}) + \frac{1}{2CH^2}\left(\frac{F_{24} + F_{25} R_o^{*2}}{F_{27}} - \frac{F_{24} + F_{25} R_i^{*2}}{\overline{F}_{27}}\right)$$
$$+ 0.5\,F_{26}\,\mathrm{Ln}\left(\frac{a - \mathrm{DR}_o^{*2}}{a - \mathrm{DR}_i^{*2}}\right) - 0.5\,\overline{F}_{26}\,\mathrm{Ln}\left(\frac{\overline{a} + \mathrm{DR}_o^{*2}}{\overline{a} + \mathrm{DR}_i^{*2}}\right)$$

$$X = 1 + \frac{2\mathrm{Br} F_{28}}{R_o^{*2} - R_i^{*2}}$$

$$\overline{\Phi} = 0.5\left(\begin{array}{l} F_{20}\,r^{*2} - F_{21}\,\mathrm{Ln}\,(r^*) + F_{22}\,\mathrm{Ln}(F_{23} - \mathrm{Dr}^{*2}) + \overline{F}_{22}\,\mathrm{Ln}(\overline{F}_{23} + \mathrm{Dr}^{*2}) \\ + F_{26}\left(\mathrm{Ln}\,(a)\,\mathrm{Ln}(r^*) - 0.5\;\mathrm{PolyLog}\left[2\;,\;\dfrac{\mathrm{Dr}^{*2}}{a}\right]\right) \\ - \overline{F}_{26}\left(\mathrm{Ln}\,(\overline{a})\,\mathrm{Ln}(r^*) - 0.5\;\mathrm{PolyLog}\left[2\;,\;-\dfrac{\mathrm{Dr}^{*2}}{\overline{a}}\right]\right) \end{array}\right)$$

$$\overline{U} = -\frac{\psi}{8}\left(\begin{array}{l} F_{11}\,r^{*2} + F_{13}\,\mathrm{Ln}\,(r^*) + F_{12}\,\mathrm{Ln}\,(a - \mathrm{Dr}^{*2}) \;+ \dfrac{\overline{F}_3\,\overline{a}\,\mathrm{Ln}\,(\overline{a} + \mathrm{Dr}^{*2})}{2D} \\ + r^{*2}\left(\begin{array}{l} 0.5\,F_1\,\mathrm{Ln}\left(\dfrac{\overline{a} + \mathrm{Dr}^{*2}}{a - \mathrm{Dr}^{*2}}\right) \\ + F_{14}\mathrm{Ln}\left(\dfrac{a - \mathrm{Dr}^{*2}}{a - \mathrm{DR}_i^{*2}}\right) + F_{15}\,\mathrm{Ln}\left(\dfrac{\overline{a} + \mathrm{Dr}^{*2}}{\overline{a} + \mathrm{DR}_i^{*2}}\right) \end{array}\right) \\ -0.5\left(\begin{array}{l} F_7\;\mathrm{PolyLog}\left[2, \dfrac{\mathrm{Dr}^{*2}}{a}\right] + \overline{F}_7\;\mathrm{PolyLog}\left[2, -\dfrac{\mathrm{Dr}^{*2}}{\overline{a}}\right] \\ + F_6\;\mathrm{PolyLog}\left[2, \dfrac{CDr^{*2}}{F_4 - F_5}\right] + \overline{F}_6\;\mathrm{PolyLog}\left[2, -\dfrac{CDr^{*2}}{F_4 + F_5}\right] \end{array}\right) \end{array}\right)$$

$$\frac{\mathrm{d}\overline{\Phi}}{\mathrm{d}r^*} = r^*\left(F_{20} + \frac{D\overline{F}_{22}}{\overline{F}_{23} + \mathrm{Dr}^{*2}} - \frac{DF_{22}}{F_{23} - \mathrm{Dr}^{*2}}\right) + \left(\frac{F_{26}\,\mathrm{Ln}\left[a - \mathrm{Dr}^{*2}\right] - \overline{F}_{26}\,\mathrm{Ln}\left[\overline{a} + \mathrm{Dr}^{*2}\right] - F_{21}}{2r^*}\right)$$

Appendix (continued)

$$\frac{\mathrm{d}\bar{U}}{\mathrm{d}r^*} = -\frac{\psi}{8}\left(\begin{array}{l} r^*\left(\begin{array}{l} 2F_{11} + \dfrac{\bar{F}_3\bar{a}}{\bar{a}+\mathrm{Dr}^{*2}} - \dfrac{2DF_{12}}{a-\mathrm{Dr}^{*2}} + F_1\mathrm{Log}\left[\dfrac{\bar{a}+\mathrm{Dr}^{*2}}{a-\mathrm{Dr}^{*2}}\right] + 2F_{14}\mathrm{Log}\left[\dfrac{a-\mathrm{Dr}^{*2}}{a-\mathrm{DR}_i^{*2}}\right] \\ +2F_{15}\mathrm{Log}\left[\dfrac{\bar{a}+Dr^{*2}}{\bar{a}+DR_i^{*2}}\right] \end{array}\right) \\ +\left(\begin{array}{l} F_7\mathrm{Log}\left[1-\dfrac{\mathrm{Dr}^{*2}}{a}\right] + \bar{F}_7\mathrm{Log}\left[1+\dfrac{\mathrm{Dr}^{*2}}{\bar{a}}\right] + F_6\mathrm{Log}\left[1-\dfrac{C\mathrm{Dr}^{*2}}{F_4-F_5}\right] \\ +\bar{F}_6\mathrm{Log}\left[1+\dfrac{C\mathrm{Dr}^{*2}}{F_4+F_5}\right] + F_{13} \end{array}\right)\Big/ r \\ +r^{*3}\left(\dfrac{2DF_{15} + F_1D(a+\bar{a})/(a-Dr^{*2})}{\bar{a}+\mathrm{Dr}^{*2}} - \dfrac{2DF_{14}}{a-\mathrm{Dr}^{*2}}\right) \end{array}\right)$$